Journal of Organometallic Chemistry 695 (2010) 1405–1413

Contents lists available at ScienceDirect

Journal of Organometallic Chemistry

journal homepage: www.elsevier.com/locate/jorganchem

Structural characterization of triorganotin(IV) complexes with sodium fusidate and DFT calculations

Michele Abbate [a], Girolamo Casella [a], Tiziana Fiore [a], Giulia Grasso [b], Claudia Pellerito [a], Michelangelo Scopelliti [a], Alberto Spinella [c], Lorenzo Pellerito [a,*]

[a] Dipartimento di Chimica Inorganica e Analitica "Stanislao Cannizzaro", Università degli Studi di Palermo, Viale delle Scienze, Ed. 17, 90128 Palermo, Italy
[b] Istituto di Biostrutture e Bioimmagini, CNR, c/o Dipartimento di Scienze Chimiche, Università degli Studi di Catania, Viale Andrea Doria 6, 95125 Catania, Italy
[c] Centro grandi apparecchiature (CGA)-UniNetLab, Università degli Studi di Palermo, Via F. Marini 14, 90128 Palermo, Italy

ARTICLE INFO

Article history:
Received 21 January 2010
Received in revised form 2 February 2010
Accepted 3 February 2010
Available online 10 February 2010

Keywords:
Steroid carboxylate
Triorganotin(IV)
NMR
FTIR
Mössbauer spectroscopy

ABSTRACT

Three new complexes of the steroid sodium fusidate (sodium 2-[(1*S*,2*S*,5*R*,6*S*,7*S*,10*S*,11*S*,13*S*,14*Z*,15*R*,17*R*)-13-(acetyloxy)-5,17-dihydroxy-2,6,10,11-tetramethyl tetracyclo[8.7.0.0^{2,7}.0^{11,15}] heptadecan-14-ylidene]-6-methylhept-5-enoate = (NaFusidate, Na**FA**)]), with triorganotin(IV) moieties have been prepared and investigated by conventional techniques as FTIR, Mössbauer, ESI-MS and NMR spectroscopy. The isolated compounds showed stoichiometries organotin(IV)/fusidate 1/1, R_3Sn(IV)**FA** (R = Me, **FA1**; Bu, **FA2**; Ph, **FA3**). The ligand coordination sites were determined by FTIR spectroscopic measurements. In the complexes, the carboxylate group of the fusidate ligand behaves as monodentate monoanionic donor, binding the Sn(IV) through one oxygen atom.

On the basis of C–Sn–O_{COO} angles, calculated through the rationalization of the ^{119}Sn Mössbauer parameter nuclear quadrupole splitting, it has been confirmed that, in all the solid state complexes, the Sn(IV) was tetracoordinated in a distorted tetrahedral structure.

Further data from ^{119}Sn CP-MAS spectra confirmed the distorted tetrahedral arrangement.

In MeOH solution, ^{1}H, ^{13}C and ^{119}Sn NMR spectroscopy showed monomeric complexes, where the carboxylate group mainly acts as monodentate ester-type ligand, and the occurrence of a coordinated solvent molecule to the tin center, as validated by non-relativistic NMR DFT study.

1. Introduction

Organotin(IV) compounds received increasing attention in the recent past years, not only because of their many and differentiate applications in industry as agricultural biocides, wood preservatives, heat stabilizers, marine antifouling paints, flame retardants, smoke suppressants, homogeneous catalysts, but also for their possible biomedical applications as antioxidants, tin-based antimicrobial drugs, potential antitumor drugs, *etc.* In this context many papers, reviews and books have been published, in the past twenty years, dealing with such applications [1–9]. Research on the synthesis and applications of metal-based drugs are currently considered as one of the most expanding areas in biomedical and inorganic chemistry [10] and very recent studies have shown very promising *in vitro* cytotoxic properties of organotin compounds [11].

Among organotin compounds, the structural chemistry of organotin carboxylates has attracted considerable attention owing to their possible structural diversity. Both di- and triorganotin carboxylates show rich and diverse structural chemistry as reported in recent publications [12–17].

Generally speaking, it has been reported that the biological behavior of organotin(IV) carboxylates is greatly influenced by the structure of the molecule and by the coordination number of the tin atom [18] and have attracted much attention due to their potential biocidal activity and cytotoxicity. In particular, steroidal organotin compounds have been synthesized and tested *in vitro* and with a parent steroid and two model compounds for further investigation on the structure–activity relationship in antitumor organotin compounds toward a series of human tumor cell lines, by M. Gielen et al. [14].

Such a strict connection between structure of organotin(IV) carboxylates and their cytotoxic [8,12,19,20] behavior stimulated in the recent past our investigations on organotin(IV) derivatives of several carboxylic acids [21–27].

Following our research interest, we chose to investigate the interaction of trialkyltin(IV) cations with steroid Na**FA**. The new

Abbreviations: **FA**$^-$, fusidate; **FA1**, Me_3Sn**FA**; **FA2**, Bu_3Sn**FA**; **FA3**, Ph_3Sn**FA**.

* Corresponding author. Tel.: +39 (0)91590367; fax: +39 (0)91 427584.
E-mail address: bioinorg@unipa.it (L. Pellerito).

0022-328X/$ - see front matter © 2010 Elsevier B.V. All rights reserved.
doi:10.1016/j.jorganchem.2010.02.001

complexes, **FA1**, **FA2** and **FA3**, have been structurally characterized in solid state by FTIR, ^{119}Sn NMR and ^{119}Sn Mössbauer spectroscopy; and by means ^{1}H, ^{13}C, ^{119}Sn NMR spectroscopy and DFT studies in methanol solution.

2. Experimental

2.1. Materials and methods

R_3SnCl (R = Me, Bu, Ph) used in the syntheses were Fluka-Riedel-de Haën (Sigma–Aldrich Company, St. Louis, MO, USA) products, while the free fusidic acid sodium salt ligand [28] (Fig. 1) was a Sigma–Aldrich Co. product. They were used without further purification.

C, H content analyses were performed in our laboratory, by using a Vario EL III CHNS elemental analyzer (Elementar Analysensysteme GmbH, Hanau, Germany). Sn content was determined in our laboratory according to standard method [29].

2.2. Synthesis of the fusidate complexes $R_3Sn(IV)FA$, (R = Me, Bu, Ph)

Sodium fusidate (0.5387 g, 1 mmol) with 1 mmol of the appropriate R_3SnCl moiety (R = Me, 0.1993 g; R = Bu, 0.27 ml, d = 1.200 g ml^{-1}, 0.3240 g; R = Ph, 0.3855 g) suspended in 50 ml of dry methanol, in the 1:1 stoichiometric ratio, were allowed to react for 24 h at about 40 °C, under a constant stirring. The resulting solution was kept in refrigerator. The precipitated NaCl was filtered off, and the solvent was removed on a rotary evaporator, and the obtained microcrystalline precipitate recrystallized twice from a 1:1 methanol:chloroform mixture. Microcrystalline precipitates obtained were not suitable for X-ray structure investigation.

Analytical data for the complexes were:

2.2.1. $Me_3Sn(IV)$***FA*** (***FA1***)

Yield 71%, m.p.: 152–154 °C, dec.; Anal. Calc. for $C_{34}H_{56}O_6Sn$: C, 60.10; H, 8.31; Sn, 17.47%; expected MW, 679.5; Found: C, 60.02; H, 8.02; Sn, 17.52%; ESI-MS: MW = 680. Positive-ion MS: *m/z* 1382 $[2M+Na]^+$; *m/z* 1219 $[M+Na\mathbf{FA}+H]^+$; *m/z* 843 $[M+Me_3Sn]^+$; *m/z* 703 $[M+Na]^+$; *m/z* 622 $[M+Na\mathbf{FA}+H+Na]^{2+}$. MS/MS of *m/z* 1382: *m/z* 703 $[M+Na]^+$. Negative-ion: *m/z* 1195 $[M+\mathbf{FA}]^-$; *m/z* 516 $[\mathbf{FA}]^-$.

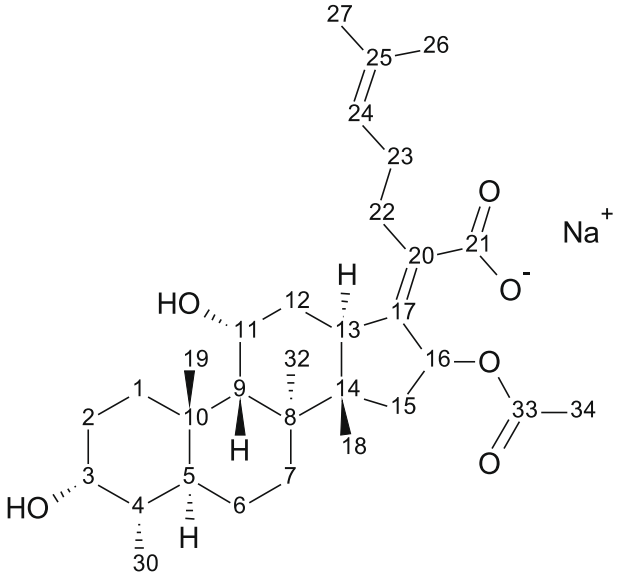

Fig. 1. Chemical structure of steroid sodium fusidate, with the numbering scheme referred to the NMR assignments (according to Ref. [28]).

2.2.2. $Bu_3Sn(IV)$***FA*** (***FA2***)

Yield 75%, m.p.: 201–203 °C, dec.; Anal. Calc. for $C_{43}H_{74}O_6Sn$: C, 64.10; H, 9.26; Sn, 14.73%; expected MW, 805.8: Found: C, 63.90; H, 9.24; Sn, 15.20%; ESI-MS: MW = 806. Positive-ion MS: *m/z* 1635 $[2M+Na]^+$; *m/z* 829 $[M+Na]^+$. MS/MS of *m/z* 1633: *m/z* 829 $[M+Na]^+$. Negative-ion: *m/z* 1322 $[M+\mathbf{FA}]^-$; *m/z* 1052 $[M+Bu_3Sn-CO_2-H]^-$; *m/z* 516 $[\mathbf{FA}]^-$.

2.2.3. $Ph_3Sn(IV)$***FA*** (***FA3***)

Yield 63%, m.p.: 207–209 °C, dec.; Anal. Calc. for $C_{49}H_{62}O_6Sn$: C, 67.98; H, 7.22; Sn, 13.70%; expected MW, 865.7; Found: C, 67.70; H, 7.04; Sn, 13.00%; ESI-MS: MW = 866. Positive-ion MS: *m/z* 1755 $[M+Na]^+$; *m/z* 889 $[M+Na]^+$. MS/MS of *m/z* 1755: *m/z* 889 $[M+Na]^+$. Negative-ion: *m/z* 1382 $[M+\mathbf{FA}]^-$; *m/z* 516 $[\mathbf{FA}]^-$.

2.3. Spectroscopic measurements

FTIR spectra were registered, as nujol and hexachlorobutadiene mulls, on a Perkin–Elmer Spectrum ONE FTIR, between CsI windows, in the 4000–250 cm^{-1} region, and in KBr pellets in the 4000–400 cm^{-1} range (Table 1).

The ^{119}Sn Mössbauer spectra (Table 2) were recorded at liquid nitrogen temperature with a multichannel analyzer (TAKES Mod. 269, Ponteranica, Bergamo, Italy) and the following Wissenschaftliche Elektronik system (MWE, München, Germany): an MR250 driving unit, an FG2 digital function generator and an MA250 velocity transducer, moved at linear velocity, constant acceleration, in a triangular waveform. The organotin(IV) samples were maintained at liquid nitrogen temperature in a Cryo NDR-1258-MD liquid nitrogen cryostat (Cryo Industries of America, Inc. Atkinson, NH, USA) with a Cryo sample holder. The 77.3 ± 0.1 K temperature was controlled with an Oxford Instruments ITC 502 temperature controller (Oxford, England). The multichannel calibration was performed with an enriched iron foil (α^{57}Fe, 4 μm, Ritverc GmbH, St. Petersburg, Russian Federation), at room temperature, by using a ^{57}Co/Rh source (10 mCi, Ritverc GmbH, St. Petersburg, Russian Federation), while the zero point of the Doppler velocity scale was determined, at room temperature, through absorption spectra of natural $CaSnO_3$ (^{119}Sn = 0.5 mg cm^{-2}) and a ^{119}Sn source (10 mCi, Ritverc GmbH, St. Petersburg, Russian Federation). The obtained $5{\cdot}10^5$ count spectra were refined, to obtain the isomer shift, $\delta \pm 0.03$ (mm s^{-1}), and the nuclear quadrupole splitting, $|\Delta_{exp}| \pm 0.02$ (mm s^{-1}).

Electrospray ionization mass spectra (ESI-MS) were recorded on a Finnigan LCQ Deca XP ion trap (Thermo Fischer Scientific, Waltham, MA, USA) using an electrospray ionization (ESI) interface. Organotin(IV)fusidate complexes were dissolved in methanol and introduced into the ESI source via a 100 μm i.d. fused silica, using a 500 μl syringe. The spectra were acquired both in the positive and negative ion mode and the instrumental conditions were as

Table 1
Assignment of more relevant absorption bands of NaFA, FA1, FA2 and FA3 in the 4000–250 cm^{-1} region.[a]

Compounds/Assignments	**NaFA**	**FA1**	**FA2**	**FA3**
ν_{OH}	3627 w 3490 s 3412 m	3441 m,bd	3465 m,bd 3407 m,bd 3315 m,bd	3385 m,bd
$\nu_{C=O}$(acetyl)	1713 vs	1720 vs	1717 vs	1713 s
$\nu_{as(COO^-)}$	1553 vs	1594 s,bd	1600 m	1596 s,bd
$\nu_{s(COO^-)}$	1385 s	1374 s	1376 s	1373 m
$\Delta\nu$ (cm^{-1})	168	220	224	223
ν_{SnC2}	–	549 s	507 w	–
Y mode	–	–	–	448 s

[a] Nujol, hexachlorobutadiene mulls and KBr pellets; s = strong, m = medium, w = weak, vw= very weak, bd = broad.

Table 2
Experimental Mössbauer parameters, isomer shift, δ, mm s^{-1}, experimental ($|\Delta_{exp}|$, mm s^{-1}) and calculated nuclear quadrupole splittings (Δ_{calcd}, mm s^{-1}), average full widths at half height (Γ_{av}, mm s^{-1}) measured at liquid N_2 temperature for triorganotin(IV) fusidates and calculated C–Sn–O_{COO} angles.

Compounds[a]	δ	$\|\Delta_{exp}\|$	Γ_{av}[b]	Δ_{calcd}[c]	C–Sn–O_{COO} angle	Proposed structure	Figure
FA1	1.27	3.21	0.76	−2.44	103	Td	2
FA2	1.42	3.09	1.16	−2.44	101	Td	2
FA3	1.20	2.34	1.02	−2.22	108	Td	2

[a] Sample thickness ranged between 0.50–0.60 mg ^{119}Sn·cm^{-2}; isomer shift, δ, ±0.03, mm s^{-1} with respect to room temperature $BaSnO_3$; nuclear quadrupole splittings, $|\Delta_{exp}| \pm 0.02$, mm s^{-1}.
[b] Γ_{av} are the average full widths at half height of the resonant peaks respect to the centroid of the Mössbauer spectra.
[c] Calculated Δ according to the point-charge model formalism applied to the idealized tetrahedral structure of Fig. 2; used p.q.s. were $([Ph]–[Cl])^{tet} = -1.26$; $([Alk]–[Cl])^{tet} = -1.37$; $([COO]–[Cl])^{tet}_{unid} = -0.15$; (unid = unidentate; tet = tetrahedral).

follows: needle voltage 4 kV; flow rate 3–5 μl min^{-1}; source temperature 200 °C; *m/z* range 50–4000.

Solid-state ^{119}Sn{^{1}H} CP-MAS spectra were obtained at 149.22 MHz on a Bruker Avance II DMX 400 MHz (9.40 T) spectrometer (Bruker BioSpin GmbH, Rheinstetten, Germany). The spectra were acquired with a number of 3000–4000 transients using recycling delays of 4 s for **FA1** and **FA2**, and 3 s for **FA3**, and contact time of 6 ms. Spinning rates of 13 KHz for **FA1**, 5 KHz for **FA2** and 12 KHz for **FA3** were used. Line broadening of 10 Hz and zero filling of 16 k points were applied to the free induction decays (FID) before transformation. After calibration on the $(cC_6H_{12})_4Sn$, a power level of 4 dB was applied in order to get the Hartman–Hahn condition.

^{119}Sn chemical shifts are given with respect to the solid $(cC_6H_{12})_4Sn$ as external reference (δ ^{119}Sn = −97.0 ppm with respect to the Me_4Sn).

One-dimensional ^{119}Sn{^{1}H} NMR spectra of MeOD solutions were recorded at 300 K on a Bruker ARX 300 (7.04 T) spectrometer at 111.92 MHz with a spectral width (SW) of 800 ppm by investigating four spectral windows with SW = 250 ppm at once in the +200 to −600 ppm range. For **FA1** a further spectrum was acquired at the same spectroscopic conditions in DMSO-d_6 solution to check the potential role of the solvent on ^{119}Sn chemical shift (δ ^{119}Sn). One-dimensional ^{1}H, ^{13}C{^{1}H} and two-dimensional ^{1}H COSY, (^{1}H–^{13}C)-gHSQC, (^{1}H–^{13}C)-gHMBC spectra in MeOD solution were acquired at 300 K on a Bruker ARX 300 (7.04 T) spectrometer at 300.13 and 76.45 MHz with a SW of 10 ppm and 200 ppm, for one-dimensional ^{1}H and ^{13}C spectra, respectively. For ^{119}Sn, Me_4Sn was employed as external reference (^{119}Sn, δ = 0.00 ppm). ^{1}H and ^{13}C resonances were calibrated on Me_4Si as external reference (^{1}H, δ = 0.00 ppm; ^{13}C, δ = 00.0 ppm). ^{119}Sn{^{1}H} and ^{13}C{^{1}H} spectra were acquired with broadband proton power-gated decoupling. For all nuclei, positive chemical shift had higher frequencies than the reference. A Lorentzian broadening of 30 Hz was applied to the FID before Fourier transformation. LW in the text is intended as line width at half height. Concentration of Na**FA**, **FA1**, **FA2** and **FA3** were *ca.* 0.07 M in MeOD solution. The concentration of **FA1** in DMSO-d_6 solution was *ca.* 0.05 M.

2.4. Computational details

Calculations were performed at the non-relativistic DFT level. Geometry optimizations for all the studied model structures (see the "Computational Study" section in Supplementary information) and Me_4Sn, used as reference for the δ ^{119}Sn calculation, were performed using the B3LYP [30,31] hybrid functional combined with the 6-31G(d,p) basis set for the H,C,O atoms and the all electron Double Zeta Valence plus Polarization (DZVP) basis set [32] for the Sn atom (contraction scheme: (18s14p9d)/[6s5p3d]). Further optimizations for **FA1** and Me_4Sn models were also done within the PCM formalism [33–35].

Calculation of the shielding constants (σ) was performed on the optimized geometries in conjunction with the Gauge Independent Atomic Orbital (GIAO) formalism by using the B3LYP hybrid functional combined with the 6-311G** basis set for the H,C,O atoms and Included Gauge Localized Orbital-II (IGLO-II) [36] as also reported in refs. [37,38]. Moreover, for comparison's sake with our previous work [39], the same calculations were also performed by using the 6-31G** basis set for the H,C,O. Calculated isotropic ^{119}Sn chemical shifts (δ_{iso}) were obtained as $\delta_{iso} = \sigma_{iso,ref} - \sigma_{iso}$, where $\sigma_{iso,ref}$ is the isotropic ^{119}Sn shielding constant of Me_4Sn and σ_{iso} is the isotropic ^{119}Sn shielding constant of the studied molecule.

$^1J(^{119}Sn,^1H)$ [^1J] and $^2J(^{119}Sn,^{13}C)$ [^2J] coupling constants for **FA1** were calculated according to ref. [40] by using the mPW1PW91 [41] hybrid functional and the 6-31G(d,p) basis set for the H, C, O atoms and the DZVP basis set for the Sn atom. All contributions to the coupling constants have been evaluated, namely: the spin-dipole (SD), diamagnetic (DSO), and paramagnetic (PSO) spin-orbit and Fermi-contact (FC) terms, whereas only the total spin-spin coupling constants are discussed in the text. For all the models the FC resulted the largest predominant contribution to the coupling constants values. Due to the size of the studied systems, suitable reduced models of **FA1** were used in the calculation of the ^1Js and ^2Js (see Fig. S1 in Supplementary information). Both for the optimizations and the NMR calculations, an integration grid of 99 radial shells and 302 angular points was used. For all calculations the software package GAUSSIAN 03 [42] was used. Cartesian coordinates of the all gas-phase optimized geometries and the SD, PSO, DSO, and FC contributions to ^1J and ^2J for **FA1** are given as Supplementary information.

3. Results and discussion

3.1. FTIR spectra

The coordination sites of the ligands were determined by FTIR spectroscopy. The most relevant absorption bands, and their assignment, both for the free and the coordinated fusidate, Fig. 1, are reported in Table 1. In particular, the invariance of the frequencies of the acetyl $\nu_{C=O}$ vibration should rule out coordination of oxygen atom of the acetyl C=O group in all of the organotin(IV)fusidate complexes. The main differences in the FTIR spectra of complexes occurred in the carboxylate stretchings. Deacon et al. [43] reported the FTIR spectra of acetate and trifluoroacetate metal complexes. The following conclusions were drawn: (i) when the $-COO^-$ group coordinates to the metal ion in a monodentate manner, the difference between the wavenumbers of the asymmetric and symmetric carboxylate stretching bands, $\Delta\nu = [\nu_{as(COO^-)} - \nu_{s(COO^-)}]$ is larger than that observed for ionic compounds. (ii) when the ligand chelates, $\Delta\nu$ is considerably smaller than that observed for ionic compounds, but for asymmetric bidentate coordination the value is in the range characteristic of monodentate coordination. (iii) The characteristic $\Delta\nu$ for the bridging bidentate ligand is larger than that for chelated ions and nearly the same as that observed for ionic compounds. On the above basis, it was

possible to distinguish between the $-COO^-$ group coordination modes.

The asymmetric and symmetric $-COO^-$ stretchings, $\nu_{as(COO-)}$ and $\nu_{s(COO-)}$, in the free sodium fusidate occurred, respectively, at 1553 and 1384 cm^{-1}, $\Delta\nu$ was equal to 168 cm^{-1}. In the $R_3Sn(IV)$-fus (R = Me, Bu, Ph) only two bands characteristic of asymmetric and symmetric $-COO^-$ stretchings are present in the FTIR spectra at around 1600 and 1375 cm^{-1}, respectively, for $\nu_{as(COO-)}$ and $\nu_{s(COO-)}$. In all the three triorganotin(IV) complexes, the $\Delta\nu$ values are larger than 200 cm^{-1} indicating an ester-type or unsymmetrical bridging carboxylate group.

Finally, bands characteristic of ν_{SnC2} and of the so-called Y mode, in the Whiffen notation [44], are present near 600 cm^{-1}, respectively in the alkyltin(IV) and phenyltin(IV) derivatives, Table 1.

3.2. $^{119}Sn\{^1H\}$ CP-MAS spectra

The $^{119}Sn\{^1H\}$ CP-MAS spectra of **FA1** (Fig. 3A) and **FA3** (Fig. 3C) showed a single broad signal at +120 ppm (LW ≈ 6300 Hz) and −118.3 ppm (LW ≈ 5000 Hz), while **FA2** (Fig. 3B) showed two relatively narrow signals with different intensity at +90.0 ppm (LW ≈ 400 Hz) and +79.2 (LW ≈ 500 Hz), respectively. All the tin chemical shift signals are in agreement with a tetracoordinated tin [45–48]. Moreover, the occurrence of a few number with low intensities side bands or, even more in the case of **FA1**, the lack of these side bands point to the loss of the tetrahedral symmetry around the tin. These findings, then, point to a heavy distortion of the ideal local tin tetrahedral arrangement expected for a tetracoordination. Finally, for **FA2** the two narrow signals indicate a long range order in solid state for this compound, being the two slight different chemical shift values due to a slight different arrangement of the tin center.

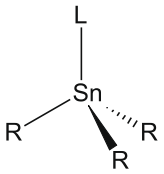

Fig. 2. Regular structure of tin assumed to estimate the nuclear quadrupole splittings according to the point-charge model formalism for four-coordinated $R_3Sn(IV)$fusidate derivatives (R = Me, Bu, Ph). The partial quadrupole splittings, p.q.s., mm s^{-1}, used in the calculations are reported in Table 3.

3.3. ^{119}Sn Mössbauer spectra

^{119}Sn Mössbauer data give an insight into the structure of the complexes in the solid state. The experimental Mössbauer parameters, isomer shift, δ (mm s^{-1}), and nuclear quadrupole splitting, $|\Delta_{exp}|$ (mm s^{-1}), of the complexes are reported in Table 2, together with Δ calculated according to the point-charge model formalism, and $C-Sn-O_{COO}$ angles for the idealized structure of Fig. 2 [49–53]. How it is evident from a comparison between experimental and calculated nuclear quadrupole splittings, Table 2, their difference exceeded, for **FA1** and **FA2**, the limit of tolerance of the method (±0.4 mm s^{-1} [53]). The rather large experimental quadrupole splitting values for **FA1** and **FA2** could be, normally, explained in terms of penta-coordination at the tin atom (probably, to form polymeric chains in the solid state), but it has also been shown that such experimental $|\Delta_{exp}|$ data can be explained satisfactorily by assuming a more or less distorted tetrahedral geometry [54]. As a consequence, taking also into account the FTIR, solid state ^{119}Sn NMR and ESI-MS data for all three aforementioned complexes, which strongly support a tetracoordination of tin(IV), we calculated the $C-Sn-O_{COO}$ angles for **FA1**, **FA2** and **FA3** derivatives according to R.V. Parish procedure [55], which confirmed, for all the complexes **FA1** and **FA2** distortion from tetrahedral structure (see Table 2) according to the bulkiness of the organic radical bonded to the tin atoms. The isomer shifts were characteristic of covalent bonds and reflected the meaning of the parameter.

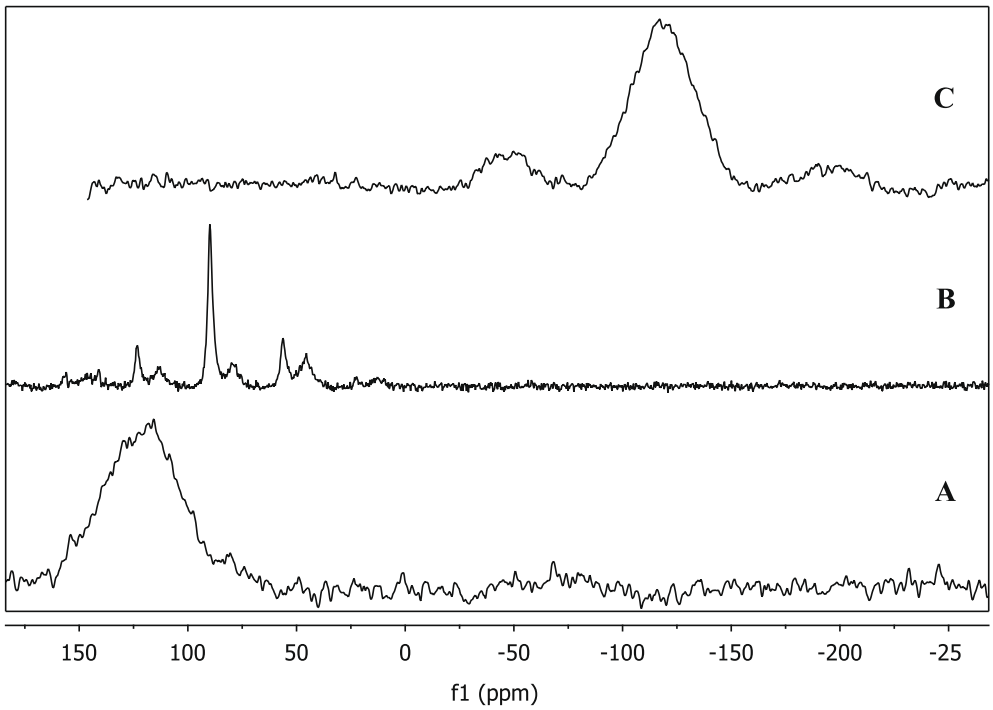

Fig. 3. $^{119}Sn\{^1H\}$ CP-MAS spectra of FA1 (A), FA2 (B), FA3 (C).

3.4. ESI-MS spectra

The ESI mass spectra of the **FA1**, **FA2** and **FA3** complexes prevalently showed the formation of monomeric and dimeric sodium adducts in agreement with organotin compounds reported in the literature [56,57] However, even if the peaks of dimeric ions showed lower relative abundances than monomeric ions in every system, their tandem mass spectra is a further contribution to confirm the molecular weights of the compounds. The assignments of the individual ions are based on the combination of positive-ion, negative-ion and tandem mass spectrometric experiments (Fig. 4a–c). These assignments were supported by comparison between theoretical and experimental isotopic distributions of monomeric $[M+Na]^+$ and dimeric ions $[2M+Na]^+$ of **FA1**, **FA2** and **FA3** compounds, the latter is reported in Fig. 4d. In particular the positive ESI mass spectra of **FA2** and **FA3** were simpler than **FA1** spectrum. In fact, the positive ESI mass spectrum of **FA1** showed monomeric and dimeric sodium peaks together with other features, probably due to the formation of adducts with trimethyltin fragment ion $[M+Me_3Sn]^+$ and Na**FA** adducts (such as $[M+Na\text{-}\mathbf{FA}+H]^+$). The negative-ion of molecule adducts with Na**FA**, $[M+\mathbf{FA}]^-$ is also observed in the spectra and support the MS assignments.

3.5. Solution-state investigation by NMR spectroscopy

In MeOD solution the $^{119}Sn\{^1H\}$ spectra of **FA1**, **FA2** and **FA3** show a single signal at +22.5 ppm (LW = 202 Hz), +31.2 ppm (LW = 527 Hz) and −194.1 ppm (LW = 110 Hz), respectively. For **FA1** and **FA2**, the δ ^{119}Sn values suggest a penta-coordination at the tin center [45–47] which could be originated from a competitive tin-(chelating)carboxylate *vs* tin-solvent interaction. In this context, despite the higher shielding effect of the butylic chains upon the δ ^{119}Sn, the more shielded value of δ ^{119}Sn observed for **FA1** with respect to the corresponding δ ^{119}Sn for **FA2**, together with their different LW values, seems to confirm the occurrence of tin/solvent interaction. Moreover, the participation of the solvent on the tin coordination is further confirmed by the

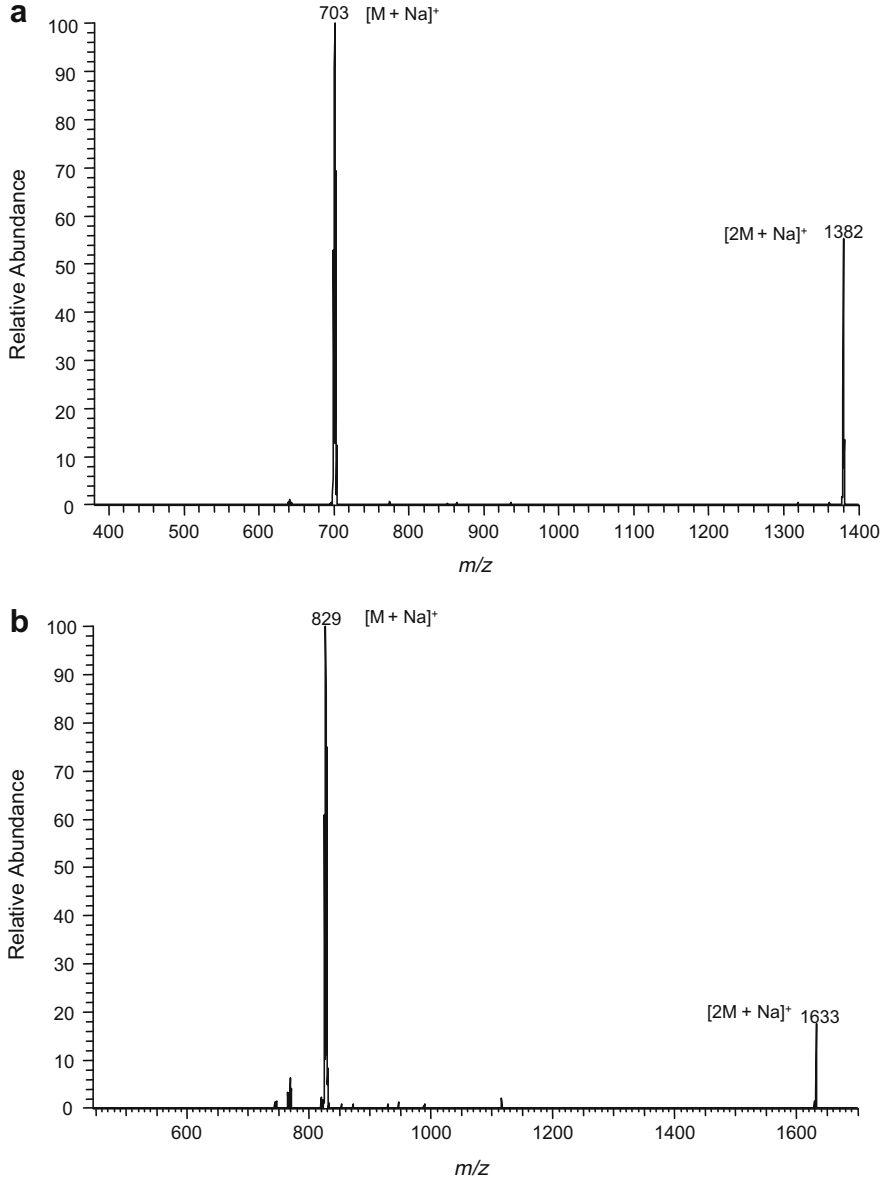

Fig. 4. Positive-ion ESI-MS/MS spectra of $[2M+Na]^+$ ion at *m/z* 1382 for FA1 compound (a), at *m/z* 1633 for FA2 compound (b) and at *m/z* 1755 for FA3 compound (c). In Fig 4d is reported positive full scan spectrum of FA3 and its zoom scan spectra of *m/z* 889 and 1755 (inset).

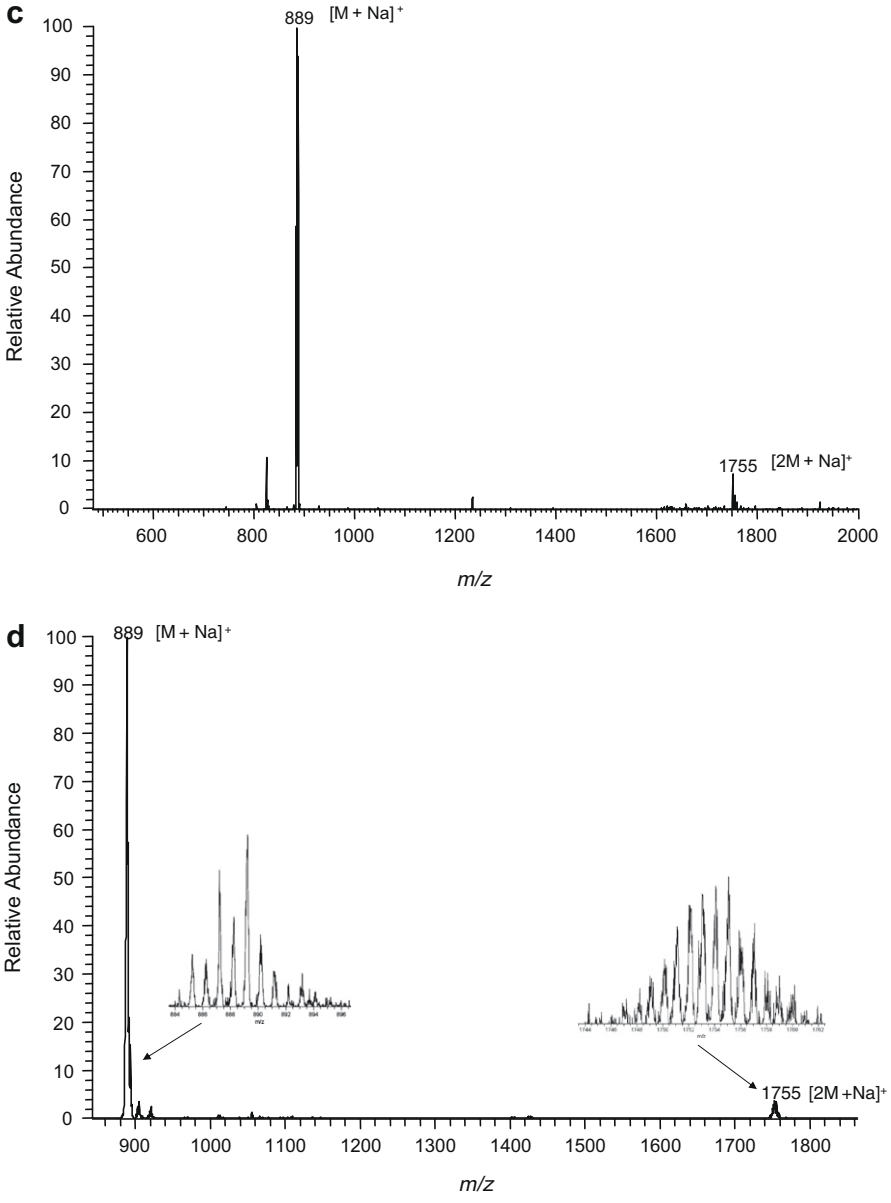

Fig. 4 (*continued*)

Table 3
Measured $^{n}J(^{119}Sn,^{13}C)$ (n = 1,2,3,4) and $^{m}J(^{119}Sn,^{1}H)$ (m = 2,3). Coupling constants are given in Hz.

Compounds	$^{1}J(^{119}Sn,^{13}C)$	$^{2}J(^{119}Sn,^{13}C)$	$^{3}J(^{119}Sn,^{13}C)$	$^{4}J(^{119}Sn,^{13}C)$	$^{2}J(^{119}Sn,^{1}H)$	$^{3}J(^{119}Sn,^{1}H)$
FA1	487.0	–	–	–	66.7	–
FA2	434.2	25.4	75.8	<7.0	n.o.	n.o.
FA3	n.o.	46.3	68.3	14.1	–	61.4

n.o. = Not observed.

−12.8 ppm δ ^{119}Sn value (LW = 224 Hz), still in agreement with a penta-coordinated tin atom, observed in DMSO-d_6 for **FA1**; this signal falls at lower frequencies with respect to the corresponding one in MeOD solution as expected being the DMSO a stronger coordinating solvent towards the tin atom. Also for **FA3**, the δ ^{119}Sn is in agreement with a penta-coordinated tin center [45–47]. In addition, for **FA3**, the observed δ ^{119}Sn value is often indicative of triphenyltin(IV)-carboxylate derivatives where the ligand acts as chelating agent and the tin atom is arranged in a *cis*-ligand-trigonal bipyramidal local geometry [58]. However, also in this case, the coordinating behavior of the solvent must to be taken into account and the participation of the solvent on tin coordination, analogously to what proposed for **FA1** and **FA2**, could not be discarded *a priori*.

The solution-state ^{1}H and ^{13}C{^{1}H} δs for **FA1**, **FA2** and **FA3** are given as Supplementary information (See Table S1). Complexation does not cause important changes in the ligands ^{1}H and ^{13}C resonances except for the ^{13}C signals corresponding to C17, C20 and

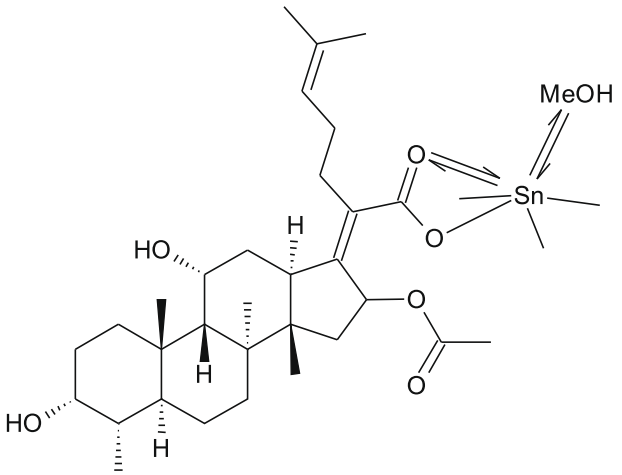

Fig. 5. Proposed configuration in methanol solution for **FA1**, **FA2**, **FA3**. The double arrows indicate the probable occurrence of the competitive exchange between the methanol and chelating carboxylate group in the tin coordination sphere. (R=Me, Bu, Ph) groups have been omitted.

C21, (with $\Delta\delta$s of 2 ppm up to 8 ppm; see Table S1 in Supplementary Information), which are indicative of the interaction of the ligand with the organotin(IV) moieties by the carboxylate group. For **FA1** and **FA2**, from the $^{1}J(^{119}Sn,^{13}C)$ and $^{2}J(^{119}Sn,^{1}H)$ satellites (Table 3), appearing in the corresponding $^{13}C\{^{1}H\}$ and ^{1}H spectra (Table 3), it was possible to estimate the C–Sn–C angle value, θ, according to the equations reported in refs [59–61]. The obtained θ values of *ca.* (117.0 ± 1.5)° and (118.0 ± 2.0)° for **FA1** and **FA2**, respectively, confirm the penta-coordination at the tin atom as inferred by the corresponding δ ^{119}Sn values (Fig. 5). For **FA3**, the δ ($^{13}C_{ipso}$) and the $^{n}J(^{119}Sn,^{13}C)$ (n = 2,3,4) values (Table 3) point to a penta-coordinated tin atom [58] still in agreement with the observed ^{119}Sn chemical shift. Moreover, it has been not possible to observe the $^{1}J(^{119}Sn,^{13}C_{ipso})$ in the $^{13}C\{^{1}H\}$ spectrum which is fundamental in discriminating if the penta-coordination at the tin center is attained by a chelating ligand, as previously mentioned, or not [58]. Nevertheless, the lack of this coupling constant in the $^{13}C\{^{1}H\}$ spectrum is indicative of the occurrence of exchanging process in solution, most probably due to the participation of the solvent on the tin coordination from which ensues that the carboxylate group should predominantly acts as monodentate ligand (Fig. 5).

3.6. NMR computational study

The NMR computational study has been performed for the R_3SnFA complexes with the aim to study the effect of the solvent

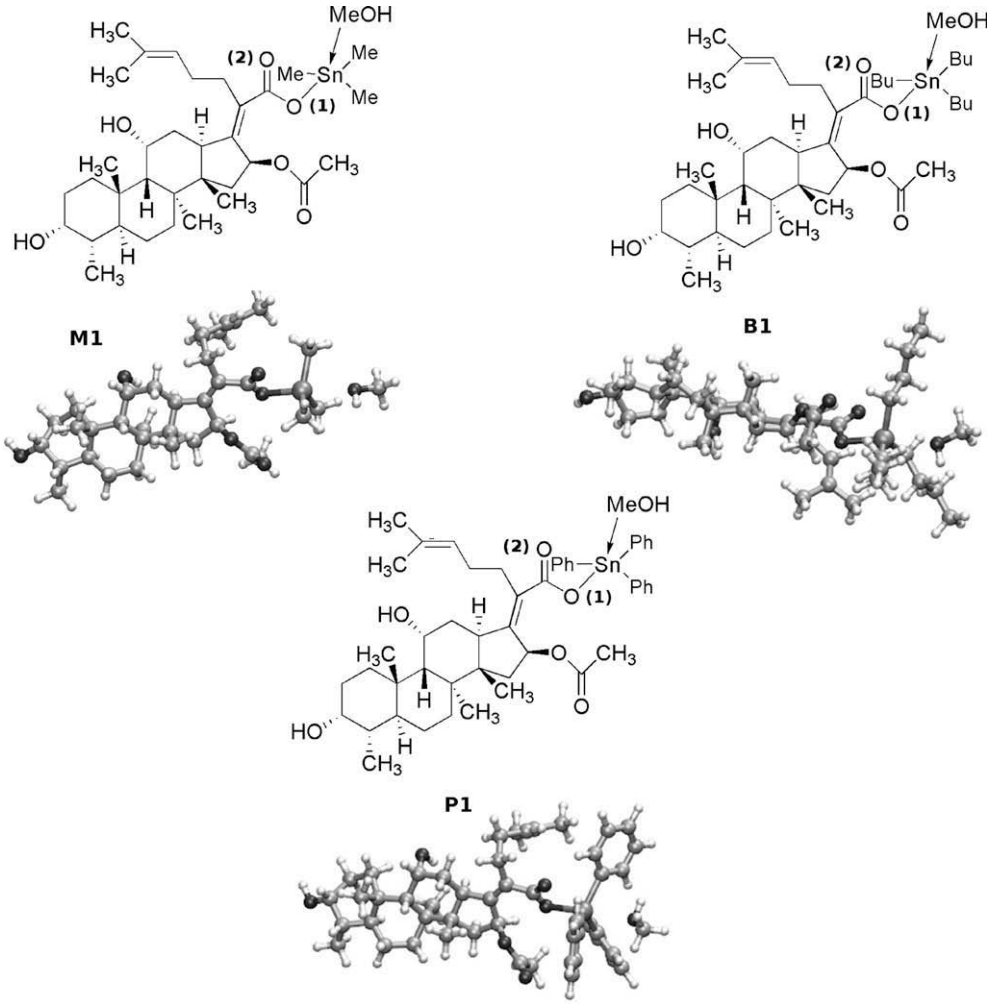

Fig. 6. Labeling of the models. The models concerning the methyl-, butyl- and phenyltin(IV) derivatives are labeled as "M", "B" and "P", respectively. The numbers "0" and "1" indicate the absence or the presence of a methanol molecule in the tin coordination sphere, respectively. In figure are reported the M1, B1 and P1 models where a solvent molecule is explicitly coordinated at the tin atom. In Table 4, a prime after the letter and/or after the number indicates that the optimization and/or the calculation of the NMR parameters have been performed within the PCM framework, respectively. The numbering of the carboxylic oxygens is also reported (see Table 4).

Table 4
Calculated θ (°), d(Sn–$O_{COO(1)}$), d(Sn–$O_{COO(2)}$) and d(Sn–O_{MeOH}) (pm), $^1J(^{119}Sn,^{13}C)$ and $^2J(^{119}Sn,^1H)$ (Hz) and δ_{iso} (ppm) for FA1, FA2, FA3. The δ_{iso} reported are referred to the data calculated with the 6-31G** basis set for the H, C, O, atoms. δ_{iso} obtained with the 6-311G** are reported as Supplementary Information.[a]

Compounds	Model	θ (°)	d(Sn–$O_{COO(1)}$); d(Sn–$O_{COO(2)}$)	d(Sn–O_{MeOH})	$^1J(^{119}Sn,^{13}C)$, Hz	$^2J(^{119}Sn,^1H)$, Hz	$\sigma_{iso,ref}$	σ_{iso}	δ_{iso}
FA1									
	Exp	117.0 ± 1.5	-	–	487.0	66.70	–	–	+23
	M0	112.6	216; 258	–	−435.5	57.51	2509.11	2444.17	+64.94
	M0′	112.6	216; 258	–	−438.2	58.03	2509.06	2443.47	+65.59
	M1	116.7	217; 270	281	−508.1	64.31	2509.11	2526.81	−17.70
	M1′	116.7	217; 270	281	−513.2	65.15	2509.06	2528.91	−19.90
FA1 (opt PCM)									
	Exp	117.0 ± 1.5	–	–	487.0	66.70	–	–	+23
	M′0	113.2	215; 264	–	−433.1	57.72	2509.26	2435.38	+73.88
	M′0'	113.2	215; 264	-	−436.6	58.36	2509.33	2433.60	+75.73
	M'1	118.1	217; 292	266	−516.9	65.82	2509.26	2529.31	−20.05
	M′1'	118.1	217; 292	266	−526.2	66.98	2509.33	2534.48	−25.15
FA2									
	Exp	118.0 ± 2.0	-	–	–	–	–	–	+31
	B0	112.7	217; 260	–	–	–	2509.11	2471.20	+37.91
	B0′	112.7	217; 260	–	–	–	2509.06	2469.57	+39.49
	B1	116.1	218; 270	293	–	–	2509.11	2519.80	−10.69
	B1′	116.1	218; 270	293	–	–	2509.06	2521.71	−12.65
FA3									
	Exp	–	–	–	–	–	–	–	−196
	P0	110.4	216; 251	–	–	–	2509.11	2681.14	−172.03
	P0′	110.4	216; 251	–	–	–	2509.06	2677.14	−168.08
	P1	115.5	217; 260	284	–	–	2509.11	2761.07	−251.96
	P1′	115.5	217; 260	284	–	–	2509.06	2757.94	−248.88

[a] θ(°) = average C–Sn–C angle; d(Sn–$O_{COO(1)}$) = distance Sn–$O_{COO(1)}$; d(Sn–$O_{COO(2)}$) = distance Sn–$O_{COO(2)}$; d(Sn–O_{MeOH}) = distance Sn–O_{MeOH}; experimental $^1J(^{119}Sn,^{13}C)$ is given as absolute value.

as well as the coordination behavior of the carboxylate group in methanol solution. For each compound, two model structures have been optimized each one differing for having none (M0, B0, P0) and one (M1, B1, P1) methanol molecule explicitly coordinated at the tin atom, respectively (see Fig. 6 for labeling of the model structures). Relevant structural data are reported in Table 4. The optimization for all the models, with none and one solvent molecule, has been started from a symmetrically coordinated chelating carboxylate group. The obtained optimized structures showed the tin atom coordinated in an asymmetric fashion by the carboxylate groups, indicating that the latter acts predominantly as monodentate ligand (See Table 4). As expected, the presence of a methanol molecule in the tin coordination sphere, which increase the electronic density at the tin nucleus, bring to an increasing in the Sn–$O_{COO(1)}$ and Sn–$O_{COO(2)}$ distances (Table 4) (see models M1, M1′, M′1, M′1′, B1, B1′, P1, P1′). This is more evident for the models concerning the **FA1** optimized with the PCM where there is a further increasing in the Sn–$O_{COO(2)}$ distances, in M′1 and M′1′ with respect to M1 and M1′ models, due to the dielectric effect of the solvent with the ensuing shortening of the Sn–O_{MeOH} distance (Table 4).

3.7. NMR parameters

The δ ^{119}Sn calculated both with the 6-311G** and the 6-31G* basis sets for the light atoms, gave similar results. In the following, taking into account that coupling constants have been calculated by using the 6-31G** basis set for the light nuclei, only the NMR parameters obtained with the latter basis set will be discussed while δ ^{119}Sn calculated with the 6-311G** are reported as Supplementary information (Table S3). For each compound, the experimental ^{119}Sn chemical shift fall between the corresponding calculated δ ^{119}Sn for the models with none and one solvent molecule pointing to the occurrence, at least from a qualitative point of view, to a dynamic interaction between the tin and the methanol. For **FA2** and **FA3** this behavior is less evident, most probably indicating a weaker tin/methanol interaction. In particular, for **FA2**, this is evident taking into account the long Sn-O_{MeOH} distance (Table 4) which could explain the experimental δ ^{119}Sn value which resulted more deshielded with respect to the δ ^{119}Sn observed for **FA1**. For **FA3**, the corresponding experimental δ ^{119}Sn is in better agreement with the calculated δ ^{119}Sn values for the model without solvent molecule and, in agreement with the relatively short calculated Sn–$O_{COO(2)}$ distance, this could implicate that the carboxylate acts mainly as chelating agent; however, the lack of the experimental $^1J(^{119}Sn,^{13}C)$, as reported above, indicating a time-dependence of these coupling, confirms the occurrence of a weak tin/methanol interaction; in addition this could be also inferred considering that the Sn–O_{MeOH} distance for **FA3** is indeed shorter than the one observed for **FA2**. The inclusion of the PCM formalism in the calculation did not strongly affect the value of the calculated δ ^{119}Sn (Table 4) confirming that the contribution of the solvent to the δ ^{119}Sn is mainly due to the methanol occurring in the first tin's coordination sphere. For **FA1** the corresponding $^1J(^{119}Sn,^{13}C)$ and $^2J(^{119}Sn,^1H)$ couplings have been also calculated. It is to note that the calculated coupling values which lie in the mean absolute error confidence range of the used protocol [40], namely: $^1J(^{119}Sn,^{13}C)_{calc} = {}^1J(^{119}Sn,^{13}C)_{exp} \pm 30$ Hz and $^2J(^{119}Sn,^1H)_{calc} = {}^2J(^{119}Sn,^1H)_{exp} \pm 2.6$ Hz, are in fairly agreement with those models where the solvent is coordinated to the tin. These findings could appear in disagreement with respect to the corresponding calculated δ ^{119}Sn which, instead, seems to indicate a solvent not strongly coordinated to the tin atom. However, these discrepancies could be imputable to different time scales involving the tin/solvent exchange process and the NMR acquisition time. Finally, also for the coupling constants, the inclusion of the PCM formalism in the M0′ and M1′ models, does not strongly affect the calculated values.

Moreover, coupling constants calculated for the **FA1** models optimized within the PCM formalism (models M′0, M′0′, M′1, M′1′) resulted substantially unchanged in magnitude, with respect to the analogous couplings for the M0, M0′, M1, M1′ models. It is worth to note that the greatest variation is observed for the $^1J(^{119}Sn,^{13}C)$s, in M′1, M′1′ models and that their values are now slightly beyond the range of confidence of the protocol used. This is imputable to the shorten Sn–O_{MeOH} distance in M′1 and M′1′

with respect to the M1 and M1′ models (Table 4) which lead to an increase of the electronic density, and then an increase in the ^1J values, as confirmed by the larger values of the corresponding FC contributions while the other contributes (DSO, PSO, SD) have been remained almost unchanged (See Table S3 in Supplementary information). However, this slight worsening of the computational protocol in the PCM framework, concerning the $^1J(^{119}Sn,^{13}C)$s, is indicative of the exchange process involving the tin and the solvent taking into account that the better performance observed for the M1 and M1′ models is correlated to the longer $Sn–O_{MeOH}$ which exceed the canonical Sn–O covalent distance [62].

4. Conclusion

Three new complexes of the steroid antibiotic sodium fusidate (NaFA) reacted in presence of methanolic solutions of the appropriate triorganotinchloride in 1:1 mole ratio resulting in complexes with stoichiometries Me_3SnFA, Bu_3SnFA and Ph_3SnFA. The FTIR, ^{119}Sn NMR CP-MAS and Mössbauer spectroscopic and ESI-MS data on the complexes revealed that the complexes are monomers and the ligand binds the metal as monoanionic monodentate ligand through the carboxylate oxygen atom so that the metal adopts a tetracoordinated more or less distorted tetrahedral (Td) geometry.

In solution phase, the experimental and calculated NMR data for the triorganotin(IV) fusidate derivatives indicate that tin is pentacoordinated and that this coordination is attained more likely considering the coordination of a solvent molecule on the tin with the ligand acting preferably as monoanionic monodentate agent.

Acknowledgments

The financial support by the Università degli Studi di Palermo (ORPA06K3RK, ORPA041443) is gratefully acknowledged.

Calculations were performed at the Computational Chemistry Centre of Palermo (CCCP) of the Dipartimento di Chimica Inorganica e Analitica “Stanislao Cannizzaro”, Università di Palermo.

Appendix A. Supplementary material

Supplementary data associated with this article can be found, in the online version, at doi:10.1016/j.jorganchem.2010.02.001.

References

[1] S.J. Blunden, P.A. Cusack, R. Hill, Industrial Uses of Tin Chemicals, Royal Society of Chemistry, Burlington House, London, London, 1985.
[2] A.J. Crowe, Appl. Organomet. Chem. 1 (1987) 143–155.
[3] A.J. Crowe, Appl. Organomet. Chem. 1 (1987) 331–346.
[4] A.J. Crowe, Antitumor activity of organotin compounds, in: S. Fricker (Ed.), Metal Compounds in Cancer Therapy, Chapman and Hall, London, 1994, pp. 147–179.
[5] M. Gielen, A.G. Davies, K. Pannell, E. Tiekink, Tin Chemistry: Fundamentals Frontiers and Applications, John Wiley & Sons, New York, 2008.
[6] E. Arkis, D. Balköse, Polym. Degrad. Stab. 88 (2005) 46–51.
[7] A.K. Saxena, F. Huber, Coord. Chem. Rev. 95 (1989) 109–123.
[8] L. Pellerito, L. Nagy, Coord. Chem. Rev. 224 (2002) 111–150.
[9] A.G. Davies, Organotin Chemistry, Wiley-VCH, Weinheim, 2004.
[10] S.K. Hadjikakou, N. Hadjiliadis, Coord. Chem. Rev. 253 (2009) 235–249.
[11] M. Gielen, E.R.T. Tiekink, Tin compounds and their therapeutic potential, in: M. Gielen, E.R.T. Tiekink (Eds.), Metallotherapeutic Drugs and Metal-Based Diagnostic Agents: The Use of Metals in Medicine, John Wiley & Sons, Chichester, 2005, pp. 421–439.
[12] S. Tabassum, C. Pettinari, J. Organomet. Chem. 691 (2006) 1761–1766.
[13] H.D. Yin, F.H. Li, L.W. Li, G. Li, J. Organomet. Chem. 692 (2007) 1010–1019.
[14] M. Gielen, M. Biesemans, D. de Vos, R. Willem, Inorg. Biochem. 79 (2000) 139–145.
[15] M. Nath, S. Pokharia, R. Yadav, Coord. Chem. Rev. 99 (2001) 215–220.
[16] V. Chandrasekhar, S. Nagendran, V. Baskar, Coord. Chem. Rev. 1 (2002) 235–240.
[17] M. Hussain, M.S. Ahmad, A. Siddique, M. Hanif, S. Ali, B. Mirza, Chem. Biol. Drug. Des. 74 (2009) 183–189.
[18] S. Shahzadi, K. Shahid, S. Ali, M. Bakhtiar, Turk. J. Chem. 32 (2008) 333–353.
[19] C. Pellerito, L. Nagy, L. Pellerito, A. Szorcsik, J. Organomet. Chem. 691 (2006) 1733–1747.
[20] M. Gielen, M. Biesemans, R. Willem, Appl. Organomet. Chem. 19 (2005) 440–450.
[21] N. Bertazzi, G. Bruschetta, G. Casella, L. Pellerito, E. Rotondo, M. Scopelliti, Appl. Organomet. Chem. 17 (2003) 932–939.
[22] A. Szorcsik, L. Nagy, J. Sletten, G. Szalontanai, E. Kamu, T. Fiore, L. Pellerito, E. Kalman, J. Organomet. Chem. 689 (2004) 1145–1154.
[23] A. Szorcsik, L. Nagy, A. Deàk, M. Scopelliti, Z.A. Fekete, A. Csàszàr, C. Pellerito, L. Pellerito, J. Organomet. Chem. 689 (2004) 2762–2769.
[24] C. Pellerito, P. D'Agati, T. Fiore, C. Mansueto, V. Mansueto, G.C. Stocco, L. Nagy, L. Pellerito, J. Inorg. Biochem. 92 (2005) 347–350.
[25] A. Szorcsik, L. Nagy, M. Scopelliti, A. Deák, L. Pellerito, G. Galbács, M. Hered, J. Organomet. Chem. 691 (2006) 1733–1747.
[26] N. Bertazzi, G. Casella, P. D'Agati, T. Fiore, C. Mansueto, V. Mansueto, C. Pellerito, L. Pellerito, M. Scopelliti, Appl. Organomet. Chem. 22 (2008) 389–396.
[27] T.S. Basu Baul, A. Paul, L. Pellerito, M. Scopelliti, P. Singh, P. Verma, D. de Vos, Invest. New Drugs, doi:10.1007/s10637-009-9293-x.
[28] J. Barber, L. Lian, G.A. Morris, M.H. Tehrani, Magn. Res. Chem. 27 (1989) 740–747.
[29] W.P. Neumann, The Organic Chemistry of Tin, Interscience, London, 1970.
[30] P.J. Stephens, F.J. Devlin, C.F. Chabalowski, M.J. Frisch, J. Phys. Chem. 98 (1994) 11623–11627.
[31] R.H. Hertwig, W. Koch, Chem. Phys. Lett. 268 (1997) 345–351.
[32] N. Godbout, D.R. Salahub, Can. J. Chem. 70 (1992) 560–571.
[33] M.T. Cancès, B. Mennucci, J. Tomasi, J. Chem. Phys. 107 (1997) 3032–3041.
[34] M. Cossi, V. Barone, B. Mennucci, J. Tomasi, Chem. Phys. Lett. 286 (1998) 253–260.
[35] B. Mennucci, J. Tomasi, J. Chem. Phys. 106 (1997) 5151–5158.
[36] W. Kutzelnigg, U. Fleischer, M. Schindler, in: P. Diehl, E. Fluck, H. Günther, R. Kosfeld (Eds.), NMR–Basic Principles and Progress, vol. 23, Springer, Heidelberg, 1990, pp. 165–262.
[37] P. Avalle, R.K. Harris, R.D. Fischer, Phys. Chem. Chem. Phys. 4 (2002) 3558–3561.
[38] R. Vivas-Reyes, F. De Proft, M. Biesemans, R. Willem, P. Geerlings, J. Phys. Chem. A 106 (2002) 2753–2759.
[39] N. Bertazzi, G. Casella, F. Ferrante, L. Pellerito, A. Rotondo, E. Rotondo, Dalton Trans. 14 (2007) 1440–1446.
[40] G. Casella, F. Ferrante, G. Saielli, Inorg. Chem. 47 (2008) 4796–4807.
[41] Y. Zhao, D.G. Truhlar, J. Phys. Chem. A 108 (2004) 6908–6918.
[42] M. J. Frisch, G.W. Trucks, H.B. Schlegel, G.E. Scuseria, M.A. Robb, J.R. Cheeseman, J.A. Montgomery, Jr., T. Vreven, K.N. Kudin, J.C. Burant, J.M. Millam, S.S. Iyengar, J. Tomasi, V. Barone, B. Mennucci, M. Cossi, G. Scalmani, N. Rega, G.A. Petersson, H. Nakatsuji, M.Hada, M. Ehara, K. Toyota, R. Fukuda, J. Hasegawa, M. Ishida, T. Nakajima, Y. Honda, O. Kitao, H. Nakai, M. Klene, X. Li, J.E. Knox, H.P. Hratchian, J.B. Cross, V. Bakken, C. Adamo, J. Jaramillo, R. Gomperts, R.E. Stratmann, O. Yazyev, A.J. Austin, R. Cammi, C. Pomelli, J.W. Ochterski, P.Y. Ayala, K. Morokuma, G.A. Voth, P. Salvador, J.J. Dannenberg, V.G. Zakrzewski, S. Dapprich, A.D. Daniels, M.C. Strain, O. Farkas, D.K. Malick, A.D. Rabuck, K. Raghavachari, J.B. Foresman, J.V. Ortiz, Q. Cui, A.G. Baboul, S. Clifford, J. Cioslowski, B.B. Stefanov, G. Liu, A. Liashenko, P. Piskorz, I. Komaromi, R.L. Martin, D.J. Fox, T. Keith, M.A. Al-Laham, C.Y. Peng, A. Nanayakkara, M. Challacombe, P.M.W. Gill, B. Johnson, W. Chen, M.W. Wong, C. Gonzalez, J.A. Pople, GAUSSIAN 03, Revision D.02; Gaussian, Inc., Wallingford CT, 2004.
[43] G.B. Deacon, F. Huber, R.J. Phillips, Inorg. Chim. Acta 104 (1985) 41–45.
[44] D.H. Whiffen, J. Chem. Soc. (1956) 1350–1356.
[45] P.J. Smith, A.P. Tupčiauskas, Ann. Rep. NMR Spectrosc. 8 (1978) 291–370.
[46] B. Wrackmeyer, Annu. Rep. NMR Spectrosc. 16 (1985) 73–186.
[47] B. Wrackmeyer, Annu. Rep. NMR Spectrosc. 38 (1999) 203–264.
[48] A. Sebald Chapter 5, in: M. Gielen, R. Willem, B. Wrackmeyer (Eds.), Advanced Applications of NMR to Organometallic Chemistry, John Wiley & Sons, Chichester, 1996, pp. 123–156.
[49] G.M. Bancroft, R.H. Platt, Adv. Inorg. Chem. Rad. 15 (1972) 59–68.
[50] R.L. Collins, J.C. Travis, The electric field gradient tensor, in: I.J. Gruverman (Ed.), Mössbauer Effect Methodology, vol. 3, Plenum Press, New York, 1967, pp. 123–161.
[51] G.M. Bancroft, V.G. Kumar Das, T.K. Sham, M.G. Clark, J. Chem. Soc., Dalton Trans. (1976) 643–654. and references therein..
[52] T.K. Sham, G.M. Bancroft, Inorg. Chem. 14 (1975) 2281–2284.
[53] M.G. Clark, A.G. Maddock, R.H. Platt, J. Chem. Soc., Dalton Trans. (1972) 281–290.
[54] R.V. Parish, Structure and Bonding in Tin Compound, in: G.J. Long (Ed.), Mössbauer Spectroscopy Applied to Inorganic Chemistry, vol. 1, Plenum Press, New York, 1984, pp. 544–548.
[55] P. Ganis, G. Valle, D. Furlani, G. Tagliavini, J. Organomet. Chem. 302 (1986) 165–170.
[56] T.S. Basu Baul, K.S. Singh, M. Holcapek, R. Jirasko, E. Rivarola, A. Linden, J. Organomet. Chem. 690 (2005) 4232–4242.
[57] T.S. Basu Baul, C. Masharing, G. Ruisi, R. Jirasko, M. Holcapek, D. de Vos, D. Wolstenholme, A. Linden, J. Organomet. Chem. 692 (2007) 4849–4862.
[58] J. Holeček, M. Nádvorník, K. Handlíř, A. Lyčka, J. Organomet. Chem. 241 (1983) 177–184.
[59] T.P. Lockhart, W.F. Manders, Inorg. Chem. 25 (1986) 892–895.
[60] J. Holeček, A. Lyčka, Inorg. Chim. Acta 118 (1986) L15–L16.
[61] T.P. Lockhart, W.F. Manders, J. Am. Chem. Soc. 109 (1987) 7015–7020.
[62] J.A. Zubieta, J.J. Zuckerman, Prog. Inorg. Chem. 24 (1978) 251–475.